Probing the circumstellar structures of T Tauri stars and their relationship to those of Herbig stars

Jorick S. Vink[1], Janet E. Drew[1], Tim J. Harries[2], René D. Oudmaijer[3], Yvonne Unruh[1]

[1] *Imperial College of Science, Technology and Medicine, Blackett Laboratory, Prince Consort Road, London, SW7 2BZ, UK*
[2] *School of Physics, University of Exeter, Stocker Road, Exeter EX4 4QL, UK*
[3] *The School of Physics and Astronomy, E C Stoner Building, Leeds, LS2 9JT, UK*

ABSTRACT

We present Hα spectropolarimetry observations of a sample of 10 bright T Tauri stars, supplemented with new Herbig Ae/Be star data. A change in the linear polarisation across Hα is detected in most of the T Tauri (9/10) and Herbig Ae (9/11) objects, which we interpret in terms of a compact source of line photons that is scattered off a rotating accretion disk. We find consistency between the position angle (PA) of the polarisation and those of imaged disk PAs from infrared and millimetre imaging and interferometry studies, probing much larger scales. For the Herbig Ae stars AB Aur, MWC 480 and CQ Tau, we find the polarisation PA to be perpendicular to the imaged disk, which is expected for single scattering. On the other hand, the polarisation PA aligns with the outer disk PA for the T Tauri stars DR Tau and SU Aur and FU Ori, conforming to the case of multiple scattering. This difference can be explained if the inner disks of Herbig Ae stars are optically thin, whilst those around our T Tauri stars and FU Ori are optically thick. Furthermore, we develop a novel technique that combines known inclination angles and our recent Monte Carlo models to constrain the inner rim sizes of SU Aur, GW Ori, AB Aur, and CQ Tau. Finally, we consider the connection of the inner disk structure with the orientation of the magnetic field in the foreground interstellar medium: for FU Ori and DR Tau, we infer an alignment of the stellar axis and the larger magnetic field direction.

Key words:
stars: formation – stars: pre-main sequence – stars: T Tauri – circumstellar matter – techniques: polarimetric

1 INTRODUCTION

We present Hα spectropolarimetry of T Tauri stars as a follow-up study of our earlier paper on the circumstellar structure of Herbig Ae/Be stars (Vink et al. 2002). Spectropolarimetry is a powerful tool to probe the inner regions around pre-main sequence (PMS) stars. Quantifying the geometry and optical depth of the gaseous inner regions of such objects is crucial for studies of planet formation (Monnier et al. 2005).

It is generally believed that low-mass stars form through the collapse of an interstellar cloud, thereby creating a circumstellar disk. During the subsequent T Tauri phase, material is accreted from the disk onto the star, most likely through magnetospheric funnels (see Johns-Krull, Valenti & Koresko 1999 and references therein). Whilst this basic picture of star formation is relatively well understood, problems relating to a star's angular momentum remain, as we

have little information on the size of the disk inner hole, the shape of the inflow and outflow or, in short, the geometry and kinematics of the circumstellar material. For intermediate mass (2 – 10 $M_\odot$) Herbig Ae/Be stars, our knowledge becomes even more patchy (see Hartmann 1999), and for stars above 10 $M_\odot$ there is not even any consensus on the mode of star formation itself (see McKee & Tan 2003).

Traditionally, the switch between low-mass and high-mass star formation has been thought to occur at the T Tauri/Herbig boundary (at $\simeq 2$ $M_\odot$), since this is where low-mass T Tauri stars possess convective envelopes, whilst intermediate mass Herbig Ae star envelopes are radiative. However, recent data indicate that such a sharp division is no longer tenable. Herbig Ae stars have a range of characteristics in common with T Tauri stars, varying from the presence of inverse P Cygni profiles, indicative of ballistic infall (Catala, Donati, & Böhm 1999), to the detections of linear

and circular line polarisations (Vink et al. 2002, Hubrig et al. 2004). These two types of line polarisations signal respectively the presence of compact line emission scattered off rotating disks, and the existence of magnetic fields for Herbig Ae stars. It is clear that what is needed to understand star formation as a function of mass (and ultimately to understand the IMF) are observations of the near-star environment over a wide range of PMS and other young stellar objects. Polarimetry across emission lines is such a tool.

The application of spectropolarimetry was first established in studies of classical Be stars (Clarke & McLean 1974; Poeckert 1975). In its simplest form, it is based on the expectation that Hα photons arise over a larger volume than the stellar continuum photons. For this reason, the line photons scatter less frequently, and over a wider range of incoming angles, off the electrons in the disk. Hence the emission line flux will be less polarised than the continuum. In this situation, a *smooth* change in polarisation across the line profile occurs: depolarisation. The high incidence of such depolarisations among classical Be stars (26 out of 44 in Poeckert & Marlborough 1976) indicated that the envelopes of classical Be stars are not spherically symmetric, and these findings are now taken as proof that classical Be stars are embedded in circumstellar disks (e.g. Dougherty & Taylor 1992; Wood, Bjorkman & Bjorkman 1997; Quirrenbach et al. 1997).

In recent years, the technique has been applied to PMS Herbig Ae/Be stars (Oudmaijer & Drew 1999; Vink et al. 2002). We have found that for the Herbig Be stars the frequency[1] of line effects (7/12) as well as its character (the above described "depolarisation" effect) hint at the presence of undisrupted disks around these objects. For the Herbig Ae stars, we found rather different Hα polarisation results. Here, the frequency was somewhat higher (9/11), and most intriguing was that the polarisation changes across Hα were narrower than the width of the intensity profile itself – which is inconsistent with depolarisation. Instead, the data show intrinsic *line* polarisations that are caused by Hα photons from a compact source that scatter off an exterior medium. In contrast to the depolarisations in the Herbig Be stars, these line polarisations seen in Herbig Ae stars yield kinematic information. The rotations in the position angle (PA) of the polarisation across the line profile translate into "loops" when the data are plotted in the Stokes QU plane. These QU loops directly imply the presence of envelope rotation (Wood, Brown & Fox 1993; Vink, Harries & Drew 2005) and suggest the existence of rotating accretion disks, similar to those accepted to be present in the lower mass T Tauri counterparts.

Given the presumed similarities between Herbig Ae stars and T Tauri stars, we presented the first medium resolution ($R \simeq 9\,000$) Hα spectropolarimetry of a T Tauri star: RY Tau (Vink et al. 2003). The observed QU loop in RY Tau showed the presence of an inner rotating disk, which is consistent with the results of longer wavelength imaging studies (Koerner & Sargent 1995) that probe the disk on larger spatial scales. In addition, our data provided a strong link between this classical T Tauri star of spectral type F8,

and the earlier-type Herbig Ae stars, where these QU loops are found to be common (Vink et al. 2002).

For the even later type (G-K) T Tauri stars narrow-band linear polarimetry has been performed (e.g. Bastien 1985), but no polarisation changes have been found to date. This could be due to a lack of sufficient spectral resolution in the older data. Our example of medium-resolution ($R \simeq 9\,000$) line polarimetry on RY Tau has shown that degrading the resolution can "wipe out" line polarisation changes (Vink et al. 2003). We note that the presumed absence of Hα polarisation features has often been used to argue that polarisation in T Tauri stars is simply due to scattering off dust – rather than off gas. Our above-mentioned data on RY Tau suggest that such a conclusion is premature, and that with the higher spectral resolution currently available, we may have to readdress these original deductions.

Furthermore, to be able to study the general relationship between Herbig Ae and T Tauri stars, it is crucial to observe more than just one T Tau star at the relatively early spectral type F8. We will see that although the line polarimetry of T Tauri stars harbours a variety of characteristics, the general behaviour is a predominance of QU loops, similar to those present in Herbig Ae stars. We supplement the T Tauri data with new (higher quality) Herbig Ae/Be star data, but the comparison between the T Tauri stars presented here and the Herbig Ae/Be stars is mostly based on the Herbig data presented in Vink et al. (2002).

An important quantity we may be able to obtain from medium-resolution ($R \simeq 9\,000$) spectropolarimetry across emission lines of PMS stars is that of the intrinsic PA of the polarisation. For an optically thin, single-scattering disk, the expected intrinsic PA of the polarisation is expected to be perpendicular to the disk PA (e.g. Brown & McLean 1977). Instead, for an optically thick, multiple scattering disk, the PA of the polarisation is expected to be parallel to the PA of the imaged disk (e.g. Angel 1969).

Spectropolarimetry can also be used to set constraints on the radii of disk inner rims. A novel technique was recently introduced by Vink et al. (2005). Their Monte Carlo scattering predictions show a difference in the wavelength dependence of the PA across emission line profiles for the case of an undisrupted disk versus one with an inner hole. This behaviour can be used to constrain the radii of disk inner holes.

Last but not least, from measured excursions in the QU plane, one may determine the direction of polarisation in the foreground of the PMS star, and obtain information on the orientation of the magnetic field in the foreground medium, and thereby gain insight into the star formation process itself.

The paper is organised as follows. In Sect. 2 we discuss how the observations were obtained. In Sect. 3, we present the general results on the continuum and line polarimetry. We then describe the data for the individual T Tauri stars, in combination with the results obtained from other techniques (Sect. 4). Complementary data on Herbig Ae/Be stars are found in Sect. 5. The two object classes are compared in Sect. 6, where we discuss the main outcomes of our study, before we conclude in Sect. 7.

---

[1] Note that a disk that is observed exactly face-on is circular on the sky and will not yield polarisation

Table 1. Targets. The *V*-band magnitudes (unless the *B*-band is specified) are taken from SIMBAD, and listed in column (2). The Spectral types (column 3) are taken from the Herbig & Bell (HB) catalogue, unless they have been improved, when they are footnoted. The T Tauri type (from HB) is given in column (4). The integration times (column 6) denote the total exposures. The continuum PA and its error are indicated in column (8), whilst column (9) indicates whether we have good Hα line polarisation data; the + indicates there is a plot of the epoch. Finally, column (10) indicates a measure of the disk PA derived from line excursions.

Name	V	Spec. Tp	Type of object	Date	Exposure(s)	$P_{\mathrm{cont}}^{\mathrm{R}}$ (%)	$\Theta_{\mathrm{cont}}^{\mathrm{R}}$ (°)	Hα data?	$\Theta_{\mathrm{intr}}^{\mathrm{R}}$
(1)	(2)	(3)	(4)	(5)	(6)	(7)	(8)	(9)	(10)
RY Tau	10.2	F8[1]	ctts	26-12-01	4×120,12×180	3.156 ± 0.007	14.7 ± 0.1	yes	163°
				10-12-03	8×120,20×240	0.831 ± 0.005	27.9 ± 0.2	yes	
				12-12-03	8×90,12×180	2.204 ± 0.004	9.3 ± 0.0	yes	
				13-12-03	8×120,12×180	2.064 ± 0.004	8.8 ± 0.1	yes	
T Tau	9.6B	K0[2]	ctts	27-12-01	8×45,16×120	0.663 ± 0.009	94.5 ± 0.4	yes +	
				12-12-03	4×60,16×150	1.133 ± 0.004	88.8 ± 0.1	yes +	
SU Aur	9.2	G2	su aur	27-12-01	12×180	0.930 ± 0.008	104.9 ± 0.2	yes	
				10-12-03	8×90,16×150	0.510 ± 0.004	99.0 ± 0.2	yes	
				11-12-03	4×90, 5×240	0.590 ± 0.002	102.0 ± 0.1	yes +	130°
				13-12-03	12×120	0.512 ± 0.006	99.0 ± 0.3	yes	
FU Ori	8.9	G3	fu ori	27-12-01	4×20	0.770 ± 0.038	132.1 ± 1.4	no	
				11-12-03	8×60	0.659 ± 0.009	129.6 ± 0.4	yes +	45°
CO Ori	10.6	F7[1]	su aur	27-12-01	8×120,8×180	2.007 ± 0.014	168.9 ± 0.2	yes	
				12-12-03	4×60	2.506 ± 0.068	159.2 ± 0.8	yes +	(60)°
DR Tau	13.6	K5[1]	ctts	27-12-01	16×180	0.362 ± 0.016	142.1 ± 1.3	yes	
				12-12-03	4×60,20×180	0.285 ± 0.008	138.1 ± 0.8	yes +	120°
RW Aur A	10.3	K3[3]	ctts	10-12-03	12×150	0.636 ± 0.009	103.5 ± 0.4	yes	
				13-12-03	4×60,20×150	0.727 ± 0.006	119.2 ± 0.2	yes +	115°
GW Ori	9.9	G5[4]	ctts	11-12-03	4×60,20×240	0.346 ± 0.003	113.8 ± 0.3	yes +	(60)°
V410 Tau	10.6	K3	wtts	12-12-03	4×90	0.206 ± 0.016	153.8 ± 2.2	no	
V773 Tau	10.7	K3	ctts	13-12-03	4×60,16×240	0.321 ± 0.004	78.8 ± 0.3	no	
UX Tau A	10.6B	K2[5]	wtts	13-12-03	4×120,24×240	0.572 ± 0.005	55.5 ± 0.3	yes +	140°
CoKu HP Tau			su aur	13-12-03	4×30	2.284 ± 0.029	65.8 ± 0.4	no	
BP Tau	10.7B	K7	ctts	13-12-03	4×30,24×300	0.102 ± 0.006	70.2 ± 1.8	yes +	

[1] Mora et al. (2001) [2] Ghez et al. (1991) [3] Rucinski (1985) [4] Bouvier & Bertout (1989) [5] Bouvier et al. (1986)

2 OBSERVATIONS

Our targets were selected from the Herbig & Bell (1988; hereafter HB) catalogue on the basis of their relative brightness ($V \lesssim 11$) and their position on the sky. We note that they were not chosen on the basis of known circumstellar geometries, or T Tauri type (i.e. classical, weak-line, naked, Fu Ori, Su Aur type, etc.). The list of objects is given in Table 1, alongside their V magnitudes and spectral types.

The linear spectropolarimetry data were obtained during the nights of 2001 December 26 and 27, and 2003 December 10 – 13 with the ISIS spectrograph on the 4.2-metre William Herschel Telescope (WHT), La Palma. In general, the data from the 2003 run are of a higher quality than those from 2001, and we therefore concentrate on those from 2003. The dates and exposure times of all epochs are given in columns (5) and (6) of Table 1. Note that a majority of targets was observed on more than one occasion, to search for rotational modulation of spectropolarimetric signatures. The observations were obtained in a very similar manner to that of the Herbig Ae/Be study by Vink et al. (2002), and we refer to that paper for details. For the set-up specifics of the 2001 December run, we refer the reader to the paper on RY Tau by Vink et al. (2003), but note that the spectral resolution was similar to that of the 2003 data. For the observations taken in 2003 December, we employed a slit width of 1.0″. We used the MARCONI2 CCD detector with the R1200R grating, with a spectral range of 1000 Å, centred at

6500 Å. This set-up corresponded to a spectral resolution of $\simeq 35$ km s^{-1} around Hα – as measured from arc line fits. To be able to analyse the linearly polarised component in the spectra, ISIS was equipped with the appropriate polarisation optics, i.e. a rotating half-wave plate and a calcite block.

The data reduction was carried out using IRAF, and included the usual bias-subtraction, flat-fielding, cosmic ray removal, spectrum extraction and wavelength calibrations of both the ordinary and the extraordinary ray. These were subsequently imported into the starlink package CCD2POL. The Stokes parameters Q and U were determined, leading to the percentage linear polarisation P and its PA θ:

$$P = \sqrt{(Q^2 + U^2)} \tag{1}$$

$$\theta = \frac{1}{2} \arctan(\frac{U}{Q}) \tag{2}$$

Note that a PA of 0°, i.e. North, on the sky is represented by a vector that lies parallel to the positive Q axis, whereas $\theta = 90°$ (i.e. East) is positioned in the negative Q direction. Positive and negative U axes thus correspond to position angles of respectively 45° and 135°.

The achieved accuracy of the polarisation data is in principle determined by photon-statistics only, and can be rather good (typically 0.01%). Nonetheless, the quality and the amount of data taken on spectropolarimetric standard stars is only sufficient to reach absolute accuracies of $\simeq 0.1\%$.
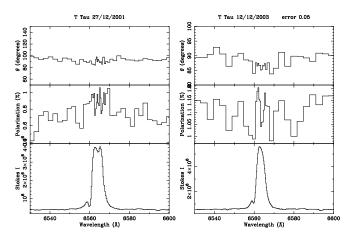
Figure 1. Triplots of the prototype T Tauri star: T Tau – at two different epochs. The total light, Stokes I, spectrum is shown in the lowest panel of the triplot, the %Pol is given in the middle panel, whilst the PA (θ; see Eq. 2) is plotted in the upper panel. The data are rebinned such that the 1σ error in the polarisation corresponds to 0.10%, as calculated from photon statistics. In case of exceptions on this, the polarisation errors are given on top of the triplots.

In most parts of the paper the polarisation spectra are shown binned to a constant error of 0.10% polarisation. Therefore, the presented spectra exhibit a resolution that depends on the number of counts at each wavelength. For this reason, the highest resolution is achieved at the wavelength of the Hα emission peak. In a few cases, we choose to modify the error per bin. This is done to achieve the best compromise between minimising the error per bin and resolving the line profile.

We do not correct for instrumental or interstellar polarisation, as these only add a wavelength-independent vector to all observed polarisations when plotted in the QU plane. Because of this wavelength independence, we generally concentrate on the QU representation of the data in classifying the type of Hα polarisation signature. We note that the instrumental polarisation is extremely low ($< 0.1\%$) with ISIS/WHT. In addition, the interstellar polarisation between us and Taurus-Auriga is also low, because of the proximity to this complex. Hence, the only significant intervening polarisation source to that of the intrinsic polarisation is that of *foreground* polarisation associated with that of the molecular cloud. The distribution of this foreground material on the sky can be patchy, and the often-used method of using the polarisations of neighbouring field stars to obtain intrinsic polarisations may lead to dubious results in the case of young stars. Instead, with line polarimetry, one can find the intrinsic PA angle *independent* of the foreground material.

Occasionally, the morphology of the excursion in the QU plane allows one to derive the direction of the foreground polarisation, and obtain the orientation of the environment's magnetic field. In such cases, the intrinsic PAs of the PMS are perpendicular to those of the foreground, which would suggest an undisturbed star-forming collapse, where the orientation of the environment's magnetic field is preserved.

3   RESULTS

We begin with a brief presentation of our continuum polarisation results (Sect. 3.1), before we focus on the line polarimetry (Sect. 3.2). For many objects, repeat observations are available. Here, we concentrate on the Hα line polarimetry data from a single 2003 epoch. However, we do consider historical continuum polarimetry in the discussions of individual T Tauri stars (Section 4).

3.1   Continuum Polarimetry

The linear polarisation of PMS continua can be attributed to the scattering of stellar photons off matter within an asymmetric circumstellar geometry. In addition, there may be a foreground contribution. The polarisation of T Tauri stars is known to be variable in a variety of cases (e.g. Vardanyan 1964; Serkowski 1969; Bastien & Landstreet 1979; Hough et al. 1981; Bastien 1982; Schulte-Ladbeck 1983; Bastien 1985; Drissen, Bastien & St-Louis 1989; Ménard & Bastien 1992; Grinin, Kolotolov & Rostopchina 1995; Gullbring & Gahm 1996; Heines, Henning & Szeifert 1997; Yudin 2000; Oudmaijer et al. 2001), and it is clear that (at least part of) the polarisation is intrinsic to the source, as the foreground contribution is likely to be non-variable.

In principle, the variability of the observed continuum polarisation may be used to identify its origin. It has been suggested that rotational modulation may signal cool and hot spots on the stellar surface (e.g. Stassun & Wood 1999), but also variable extinction by a dusty disk can lead to quasi-periodic behaviour of the observed level of dust polarisation (e.g. Ménard & Bastien 1992).

Partly based on what Bastien (1982) noted as a general absence of polarisation changes across Hα in T Tauri stars, he advanced what is now the commonly accepted view on the origin of T Tauri polarisation: namely that it is due to scattering off extended dusty envelopes, where the geometry and kinematics of gas does not play a role. Whether this view represents the entire picture is a different story, as it has recently been challenged by the discovery of polarisation changes across Hα in the classical T Tauri star RY Tau (Vink et al. 2003) and the results presented here. It is therefore not yet settled which polarigenic agent causes the circumstellar polarisation in T Tauri stars. Instead, this issue should be considered open, until one can predict the polarisation of the objects, as a function of wavelength, through spectral lines, as a function of time.

The measured continuum polarisations are summarised in Table 1. The mean percentage polarisation and PA appear in columns (7) and (8). In addition, for cases where an excursion in QU space is present, we can estimate the sky PA from these line excursions, and present them in column (10). We emphasise that the presumed disks would be expected to lie orthogonal (i.e. at 90°) from this position angle, if multiple scatterings are negligible.

3.2   Hα line polarimetry

The observed Hα characteristics of each target are listed in Table 2. The first few columns list the parameters as deduced from the Stokes I profiles only: the equivalent width (EW; column 2) and the line over continuum contrast (column 3).
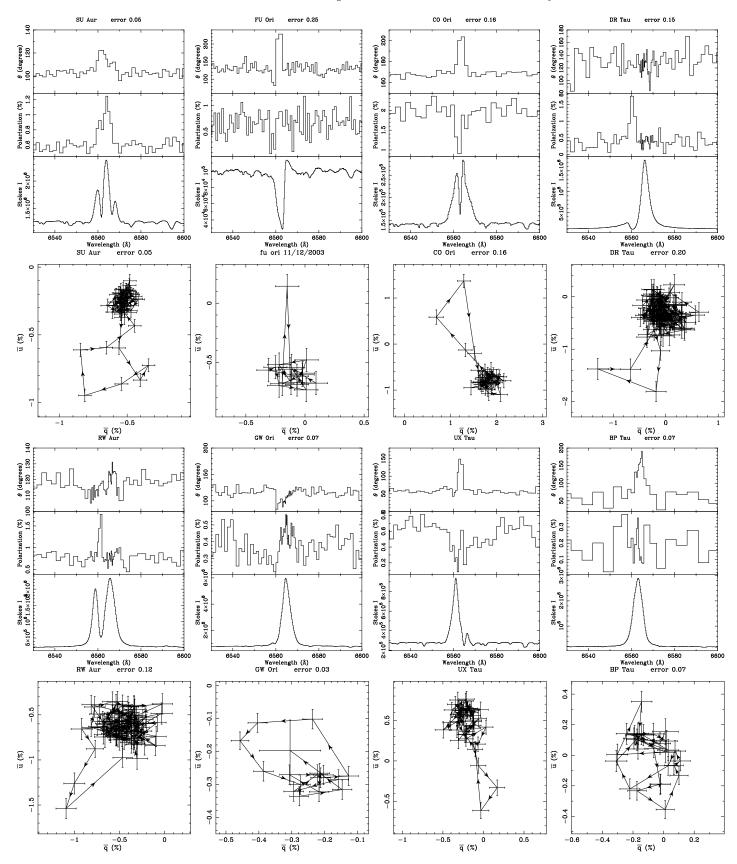
Figure 2. Polarisation spectra (see Fig. 1) of the line effect T Tauri stars and their QU diagrams (below the triplots). The lower plot represents the normalised Stokes parameters $u = U/I$ against $q = Q/I$.

Table 2. The Hα line results. The errors on the equivalent widths of the Hα lines (column 2) are below 5%, the errors on $\Delta\lambda(\mathrm{Pol})$ (column 5) and $\Delta\lambda(I)$ are determined at Full Width Zero Intensity (FWZI) and are about 10%. $\Delta\lambda(\mathrm{Pol})$ has been defined as the width over which the polarisation changes. In the case where the widths in PA and %Pol are unequal, we take the largest of the two. The fractional width ($\frac{\Delta\lambda(\mathrm{Pol})}{\Delta\lambda(I)}$) is given in Column (6). The recipe with regard to the depolarisation question (column 7) is described in the text. Column (8) represents the morphology in QU space.

Object	Hα EW(Å)	Line/Cont contrast	Line effect?	$\Delta\lambda(\mathrm{Pol})$ (Å)	($\frac{\Delta\lambda(\mathrm{Pol})}{\Delta\lambda(I)}$)	depolarisation?	QU behaviour	Mean character
(1)	(2)	(3)	(4)	(5)	(6)	(7)	(8)	(9)
RY Tau	−10	2.1	Yes	16	0.50	No	loop	Loop
	−20	3.2	Yes			No	loop	
	−14	2.6	Yes			No	loop	
	−16	2.8	Yes			No	loop?	
T Tau	−54	9.5	Yes?	–	–	Yes?	–	None
	−35	10	No	–	–	–	–	
SU Aur	−6.3	1.7	Yes			No	exc	Loop
	−7.7	2.1	Yes	15	0.60	No	loop	
	−4.6	1.9	Yes			No	loop	
	−3.9	1.5	Yes			No	loop	
FU Ori	+2.3	0.3	Yes	9	0.33	No	exc	McLean
CO Ori	−6.3	2.0	Yes			No	exc/loop?	Exc/Loop
	−49	16	Yes?	19	0.53	No	–	
DR Tau	−33	12	Yes			No	exc	McLean
	−57	15	Yes	30	0.17	No	loop?	
RW Aur A	−20	7.3	?	22	0.50	No	–	Loop/McLean
	−70	11	Yes			No	loop?	
GW Ori	−27	7.5	Yes	16	0.69	No	loop	Loop
UX Tau	−9.0	3.4	Yes	13	0.85	Yes	exc	Depol
BP Tau	−70	15	Yes	17	0.41	No	loop?	Loop

The Stokes I Hα line shapes of the target stars vary from pure emission, to P Cygni and inverse P Cygni type, through to clear double-peaked, and even more complicated line profiles. We have already seen in Vink et al. (2002) that Stokes I line profiles do not necessarily correlate with the line polarimetry, which is here confirmed. Whilst the Stokes I line profiles may vary dramatically from one object to the next, the different stars often still share similar Stokes Q and U profiles. This is illustrative of the fact that polarised light has a more selective origin than total light, in that intensity contains both direct and scattered light, whereas polarised light only contains the latter. Columns (4) to (8) in the Table concern line polarimetry properties. We note that we have only measured the widths of the line profiles for the data that we actually plot. However, we do address the line polarimetry behaviour at all epochs (in columns 7 and 8), to make the best judgement for the mean polarisation character of the object under consideration (column 9).

Contrary to our published work on the classical T Tauri star RY Tau (Vink et al. 2003), the prototype, T Tau itself, stands out in that it does not appear to show a significant line effect, cf. Fig. 1. The figure shows polarisation spectra of T Tau from both 2001 and 2003 presented as triplots (consisting of Stokes I, P, and θ). The data for all other T Tauri objects do show a significant variation in either the polarisation and/or the PA across the line, and these are presented in Fig. 2, as triplots and also as loci in the QU plane. The high number of line effect detections for T Tauri stars, 9 out of 10 (including RY Tau), is very similar to that found for Herbig Ae stars (9/11, Vink et al. 2002), and

contradicts earlier narrow-band polarimetry results, which did not have the required spectral resolution.

Although the morphology in both the polarisation triplots and QU space shows some variety between objects, we classify them according to their common characteristics, and apply the same two measures as those for Herbig Ae/Be stars (Vink et al. 2002). One measure involves the fractional line width ($\frac{\Delta\lambda(\mathrm{Pol})}{\Delta\lambda(I)}$) over which the polarisation changes (see column 6 in Table 2). The other is the description of the shape of the polarisation change across the line (columns 7 and 8). Whether or not the change in polarisation across Hα is consistent with the depolarisation mechanism is noted in column (7). The recipe followed to come to the answer is the same as that in Vink et al. (2002): if the fractional width ($\frac{\Delta\lambda(\mathrm{Pol})}{\Delta\lambda(I)}$) is larger than 0.75 and the behaviour in %Pol and PA is smooth across the line, it is consistent with depolarisation; in case the fractional width ($\frac{\Delta\lambda(\mathrm{Pol})}{\Delta\lambda(I)}$) is less than 0.75, and there is a rotation across the line profile, causing a loop in the QU plane (column 8), the behaviour is inconsistent with depolarisation and intrinsic *line* polarisation is inferred. In every case we expect to see a dark knot of points in the QU plane, which arises from the sampling of the continuum polarisation. Where there is a more or less linear excursion arising from the continuum knot, we refer to this excursion with "exc". The mean character (column 9) combines the information from the QU plane and the triplots of all available epochs.
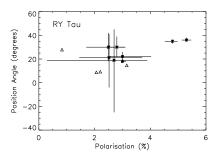
Figure 3. Plot of the current (open triangles) and previous (crosses) continuum % Pol and PA for RY Tau. Note that the large crosses do not represent error bars, but short-term polarisation variability with N measurements, where N is given in the 4th Column of Table 3.
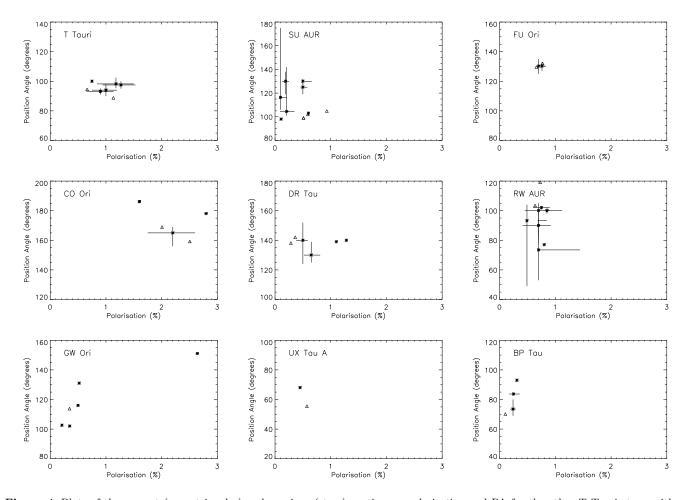

Figure 4. Plots of the current (open triangles) and previous (stars) continuum polarisation and PA for the other T Tauri stars, with the y and x-axes fixed to respectively a PA range of $100^{\rm o}$, and a % Pol of $3^{\rm o}$. Note that the large crosses do *not* represent error bars, but short-term polarisation variability over N measurements, with N given in the 4th Column of Table 3.

4   T TAURI STAR RESULTS

We searched the literature for relevant information on individual objects. Since this is the first extensive line polarimetry study on T Tauri stars, the polarisation review consists of continuum measurements only. These are plotted in Fig. 4, and summarised in Table 3. We have restricted our review to V and R bands only, and not considered wavelengths shorter than 5500 Å, or longer than 7600 Å.

In Sect. 4.1, the polarisation information is complemented with information from imaging studies. We stress that for an approximately single-scattering disk, the PA is expected to lie orthogonal to the imaged disk. For a more opaque disk however, multiple scatterings in the vertical disk direction enforce the PA to align with the disk (Angel 1969; Bastien & Ménard 1988). The imaging studies comprise both millimetre (mm) studies, and near-infrared (NIR) imaging with a coronograph, or interferometry. The information we

obtain is that of disk position angles and inclinations. The goal of the position angles is to compare them with the PAs we derive from the line polarimetry. From the inclinations, we can constrain disk inner hole sizes using the line polarimetry predictions of Vink et al. (2005). In Sect. 4.2, we change focus to the larger scale, associated with the orientation of the environment's magnetic field direction.

4.1   The inner disk results

4.1.1   RY Tau

RY Tau has a relatively low level of veiling at optical wavelengths, i.e. ≤ 0.1 (e.g. Basri, Martin & Bertout 1991), however the veiling at infrared wavelengths is markedly higher, i.e. > 0.8 (Folha & Emerson 1999). This mismatch in veiling is typical for T Tauri stars, and it suggests the object may still be actively accreting, whilst exhibiting a relatively low level of optical veiling. RY Tau has a rotational velocity of $v \sin i = 55 \pm 3$ km s^{-1} (Mora et al. 2001), but the period of 5.6 days, as reported by Herbst et al. (1987), has never been confirmed. From millimetre mapping, Koerner & Sargent (1995) infer a disk PA of $48^{\circ} \pm 5^{\circ}$, with an inclination angle $i = 25^{\circ}$. Kitamura et al. (2002) report a disk with a PA of $59^{\circ} \pm 7^{\circ}$ and an inclination angle of $i = 27^{\circ} \pm 7^{\circ}$. They also derive a disk inner radius of $R_{\mathrm{in}} = 0.14$ AU $= 10\ R_{*}$ from their modelling. Finally, Akeson et al. (2003) perform NIR interferometry, and they find a disk at a PA of $62^{\circ} \pm 10^{\circ}$ and an inclination of $i = 30^{\circ}$.

The linear percentage continuum polarisation has been reported to vary between 1 and 4%, and its PA between -20 and 45°, with %Pol $\simeq 3$ and PA $\simeq 20^{\circ}$ being typical "median" values (see Table 3).

Our data: We have measured a continuum polarisation between about 0.8 and 3.1% at a somewhat variable PA of approximately 20° (Fig. 3). This is in keeping with earlier continuum measurements. We have already reported on the line polarimetry of RY Tau in Vink et al. (2003): the line polarisation data indicate the presence of a rotating disk, and we argued for an intrinsic PA of 147° or 163°. The expected single scattering disk PAs are perpendicular to this at 57° and 73°, respectively. These angles are comparable to those derived from imaging (PA $= 62^{\circ}$).

4.1.2   T Tau

T Tau is a triple system (Dyck, Simon & Zuckerman 1982; Ghez et al. 1991; HB; Koresko 2000), and T Tau North is the optically visible prototype T Tauri star. Smirnov et al. (2003) have possibly detected a small magnetic field. The star's rotational velocity is $v \sin i = 19.5 \pm 2.5$ km s^{-1} (Bertout et al. 1986), and the rotational period is 2.80 days (Herbst et al. 1987). Hogerheijde et al. (1997) and Akeson, Koerner & Jensen (1998) detect a disk from mm observations and conclude that the disk is observed nearly face-on, i.e. at a low inclination. Johns & Basri (1995) had already claimed a low inclination for the system on the basis of the Hα correlation matrix, which was confirmed by Calvet et al. (1994) who modeled the spectral energy distribution (SED). Most recently, Akeson et al. (2002) have performed IR interferometry, confirming the

low inclination of the system: $i = 29^{\circ}{}^{+10}_{-15}$ at a PA $= 132^{\circ}{}^{+13}_{-20}$.

Our data: The line polarisation data for this star (Fig. 1) do show variability. The data from 2001 may show a weak depolarisation, but those from 2003 do not. This change may simply be due to a fall in the amount of ionised gas close to the star that can scatter and polarise the continuum photons and emit in Hα (the Hα equivalent width decreases too, cf. the discussion on the Herbig Be star MWC 166 in Vink et al. 2002). In any case, the absence or weakness of the depolarising line effect is not surprising given T Tau's pole-on orientation, as circular symmetry on the sky results in a cancellation of the polarisation vectors.

4.1.3   SU Aur

The relatively massive T Tauri star SU Aur has an uncertain period of in between 1.7 (DeWarf et al. 2003) and 2.7 days (Herbst et al. 1987; Unruh et al. 2004). The rotational velocity is $v \sin i = 59 \pm 1$ km s^{-1}. Akeson et al. (2002) image a disk at a PA of $127^{\circ}{}^{+8}_{-9}$. They derive an inclination of $i = 62^{\circ}{}^{+4}_{-8}$, which is consistent with the Doppler imaging studies of Petrov et al. (2001) and Unruh et al. (2004) which also favour i between 50° and 70°. Akeson et al. (2002) also model the disk inner rim and find a hole of radius 0.05 – 0.08 AU, which corresponds to $\simeq 2.7$ – 4.3 stellar radii. This compares well with the expected corotation radius of 2.5 – 3 stellar radii.

Our data: We have measured a continuum polarisation between about 0.5 and 0.9% at a more or less fixed PA of $\simeq 100^{\circ}$. Although the PA is variable, the 100° seen here appears to be common for this object, since it generally experiences a PA in the range 100° – 130°.

The single QU loop, at a preference PA of $\simeq 120^{\circ}$, may highlight two issues. First, the PA of the intrinsic polarisation aligns with the PA found from mm imaging, which would suggest the presence of an optically thick multi-scattering envelope, such that the PA of the polarisation aligns with the disk PA.

Second, the sheer presence of a *single* loop suggests the presence of a disk inner hole. This deduction is based on the Monte Carlo models by Vink et al. (2005) which show that there is a marked difference in polarisation changes across line profiles of line emission originating from a point source – resembling a situation where the photons are scattered off a disk with a large inner hole – and a finite-sized star – where the inner hole is small. In between these two extremes, there is transitional behaviour which can also be used to constrain the size of the disk inner hole, provided the disk inclination is known. Since SU Aur is a system with a well-known inclination, $i \simeq 60^{\circ}$, we can use the predictions by Vink et al (2005) to estimate a lower limit to the disk inner radius: $R_{\mathrm{in}} > 3\ R_{*}$. This is consistent with the inner radius found by Akeson et al. (2002).

4.1.4   FU Ori

FU Ori is the prototype of the outbursting low mass young stellar objects. These stars show large increases in optical brightness of $\simeq 5$ magnitudes on timescales ranging from less

than a year, to more than a decade (e.g. Herbig 1977). The frequency of these outbursts is uncertain, but it is believed that these outbursts may represent the principal mode of accretion onto young stars (e.g. Hartmann & Kenyon 1985). The deeply seated P Cygni absorption is usually interpreted as being due to an almost pole-on system. Recently, Wang et al. (2004) have detected a faint red star in the apparent vicinity of FU Ori. This is possibly a close companion at a PA of $161^{\circ} \pm 3^{\circ}$ with a separation of about 225 AU.

Malbet et al. (1998) resolved FU Ori, but could not unravel its morphological structure. They also modelled the SED, and found an inclination of 30°. More recently, Malbet et al. (2005) have performed 2.2 μm interferometry, and they now find actual physical parameters for the disk PA and inclination, using two different models. In the first model (disk only), the PA is $47^{\circ} \pm 10^{\circ}$ and $i = 55^{\circ} \pm 7^{\circ}$. In the second model (a disk and a bright spot), they find a PA of $8^{\circ} \pm 21^{\circ}$ and $i = 46^{\circ} \pm 10^{\circ}$.

Our data: We have measured a continuum polarisation of about 0.7% at a PA of approximately 130°. It appears that the level of %Pol as well as the PA remain constant. Despite the low S/N, the line polarimetry shows a clear occurrence of the "McLean effect" (McLean 1979), where blue-shifted line absorption (in Stokes I) is accompanied by a change in the polarisation percentage and/or PA over its width. This change in polarisation/PA corresponds to an excursion in the QU plane at $\simeq 45$ degrees, which defines the intrinsic plane of the continuum polarisation (independent of foreground polarisation). The reasoning is that the blue-shifted absorption mostly removes direct stellar continuum light, which is unscattered and unpolarised. As a result, the (few) blue-shifted photons that do reach the observer are selectively more polarised, defining the intrinsic plane of continuum polarisation. Since the disk of FU Ori is optically thick, with a high accretion rate (of up to 10^{-4} $M_{\odot}$ yr^{-1}), we would expect the PA of the optically thick disk on the sky to align with the PA from the line excursion. It appears that the PA we derive from the QU plane is consistent with the PA of $47^{\circ} \pm 10^{\circ}$ from the disk model by Malbet et al (2005).

4.1.5 CO Ori

Despite its relative brightness, CO Ori appears to be poorly studied. Reipurth et al. (1996) note that the pronounced P Cygni profile of CO Ori (not seen in our data) is reminiscent of FU Ori, as well as its relatively early spectral type.

Our data: We have measured a continuum polarisation of about 2.0% at a PA of approximately 160°, which is consistent with earlier continuum measurements (Table 3, Fig. 4). Despite the relatively low S/N, we tentatively infer an intrinsic PA of $\simeq 60^{\circ}$ from the excursion in the QU plane. When the larger scale disk of this object will be imaged, we expect the imaged disk to have a PA of $\simeq 60^{\circ}$, if it is an optically thick, multiple scattering disk.

4.1.6 DR Tau

DR Tau exhibits strongly variable emission lines (e.g. Smith et al. 1999) which may signal both inflow and outflow. The

Balmer lines are strongly asymmetric, peaking in the red, and do not resemble magnetospheric infall model predictions. Alencar, Johns-Krull & Basri (2001) propose the system is observed nearly pole-on, but Muzerolle, Calvet & Hartmann (2001) suggest a high inclination ($i = 70^{\circ}$), and advocate a scenario in which most of the Hα is formed in the stellar wind, rather than in the accretion flow. The mm imaging data of Kitamura et al. (2002) seem to support the more edge-on viewing angle: $i \simeq 67^{\circ}$ at a PA of $\simeq 128^{\circ}$. They estimate a disk radius of about 200 AU, and they derive an inner radius of 10 R_* based on disk models. Kravtsova & Lamzin (2002) argue that $i < 60^{\circ}$, and Greaves (2004) models the HCO$^+$ lines, and she finds an inclination between $4 - 9^{\circ}$. These results appear to be in contradiction to the mm study by Kitamura et al. However, based on all other evidence, such as the low rotational velocity, $v \sin i < 10$ km s^{-1}, the period of 5.1 days (Johns & Basri 1995) and the stellar size, we consider the more pole-on orientation to be more plausible.

Our data: We have measured a continuum polarisation of about 0.3% at a PA of approximately 140° (consistent with earlier continuum measurements, cf. Table 3).

The line polarimetry data show the occurrence of the "McLean effect", where blueshifted line absorption (in Stokes I) is accompanied by a change in the %Pol/PA over the same wavelength region as the P Cygni absorption (cf. the case of FU Ori). From the loop in the QU plane, we infer an intrinsic PA of $\simeq 120$ degrees for the system, which is in good agreement with the PA of 128° found by Kitamura et al.

4.1.7 RW Aur A

RW Aur is a resolved triple system (Ghez, Neugebauer & Matthews 1993) with RW Aur A dominating the optical light. The star has a rotational velocity of $v \sin i = 19.5 \pm 4.6$ km s^{-1} (Hartmann et al. 1986), while Petrov et al. (2001) report a photometric period of in between 2.6 and 2.9 days. López-Martín, Cabrit & Dougados (2003) infer a jet inclination angle of $\simeq 45^{\circ}$. From HST spectroscopy Gómez de Castro & Verdugo (2003) infer an inner disk radius of between 2.7 R_* and the corotation radius of 6.1 R_*.

Our data: We have measured a continuum polarisation of about 0.7% at a PA of approximately 110°.

The line polarimetry data seem to show the occurrence of the "McLean effect", here not across a bona-fide P Cygni profile, but nonetheless across envelope absorption. From the loop in the QU plane, we infer an intrinsic PA of $\simeq 115^{\circ}$ for the system. When the larger scale disk of this object will be imaged, we expect the imaged disk to have a PA of $\simeq 115^{\circ}$, if it is an optically thick, multiple scattering disk.

4.1.8 GW Ori

GW Ori is a single-lined spectroscopic binary (Murdin & Penston 1977) with a period of 242 days, in a nearly circular orbit. The system is surrounded by a massive circumbinary disk. Most of the sub millimetre light originates at 500 AU (Mathieu et al. 1995).

The star has a rotational velocity $v \sin i$ of $40 - 43$

km s^{-1}(Bouvier et al. 1986; Hartmann et al. 1986), and a period of 3.2 days (Bouvier & Bertout 1989), although this period has not been confirmed by Gahm et al. (1993). Bouvier & Bertout (1989) infer an almost pole-on orientation angle i of 15$^{\rm o}$, while Mathieu, Adams & Latham (1991) prefer $i \simeq 27^{\rm o}$, since only 26 L$_\odot$ (out of a 70 L$_\odot$ total) is believed to be stellar, with the remainder of the system's luminosity attributed to accretion. From SED modeling, Mathieu et al. (1991) derive a gap in the disk over the range of 0.17 – 3.3 AU, in broad consistency with the models of Artymowicz & Lubow (1994) who predict a disk gap between 0.45 and 2.0 AU, due to the secondary star at a distance of 1.1 AU from the primary. Najita, Carr & Mathieu (2003) derive a CO emission ring between an inner radius $R_{\rm in}$ of 0.07 AU (i.e. 3 R_*) and an outer radius of 0.6 AU, adopting $i \simeq 27^{\rm o}$.

We note that the object appears to show (quasi)-algol type eclipses, which Shevchenko et al. (1998) attributed to a high binary inclination, with Lamzin et al. (1998) reporting $i \simeq 83^{\rm o}$. For the PA of the object, Mathieu et al. (1995) report a value 56$^{\rm o}$, but warn that the object is not well-resolved.

Our data: We have measured a continuum polarisation of about 0.3% at a PA of approximately 114$^{\rm o}$. The line polarimetry data show a loop in the QU plane, possibly at an intrinsic PA of approximately 60$^{\rm o}$, which may, or may not, be consistent with the value of 56$^{\rm o}$ in Mathieu et al. (1995).

The gradual slope in the behaviour of the PA is reminiscent of the transitional PA behaviour between a finite-sized star and a point-source as predicted by Vink et al. (2005). If we assume the low inclination of 15$^{\rm o}$, and look up the transitional behaviour of the PA for this inclination in Vink et al. (2005), we find a disk inner hole size of $\simeq 4\ R_*$. For $i \simeq 27^{\rm o}$, the disk inner hole would be smaller, e.g. $\simeq 3\ R_*$, consistent with the study by Najita et al. (2003). We point out that we have assumed that the line photons originate from the primary, and that the secondary is not contributing significantly to the line emission.

4.1.9   *UX Tau A*

UX Tau A has a rotational velocity of $v\ {\rm sin}i \simeq 26$ km s^{-1}(Hartmann et al. 1986; Bouvier & Bertout 1989), and a period of 2.7 days according to Bouvier & Bertout 1989 (based on data from Mundt et al. 1983). Bouvier & Bertout (1989) also report an inclination of $50 \pm 6^{\rm o}$ for UX Tau A, but this number is most uncertain, given the uncertain period and stellar size (due to the uncertain luminosity). We have searched the literature for imaging data, but these seem to be unavailable at the present time.

Our data: We have measured a continuum polarisation of about 0.5% at a PA of approximately 65$^{\rm o}$ (in agreement with earlier measurements, cf. Table 3). We can infer an intrinsic PA of $\simeq 140^{\rm o}$ from the excursion in the QU plane. When the larger scale disk of this object will be imaged, we expect the imaged disk to have a PA of $\simeq 140^{\rm o}$, if it is an optically thick, multiple scattering disk.

4.1.10   *BP Tau*

BP Tau was the first T Tauri star found to have a large surface magnetic field (of 2.6 kGauss, Johns-Krull et al. 1999). More recently, Symington et al. (2005) find a peak longitudinal field of 4 kGauss. The star has a low rotational velocity, i.e. $v\ {\rm sin}i < 10$ km s^{-1}(Hartmann et al. 1986), but reliable periods have not yet been reported. Sub-millimetre imaging in the CO line by Simon, Dutrey & Guilloteau (2000) reveals a PA of $152^{\rm o} \pm 3^{\rm o}$, and an inclination $i = 30^{\rm o+4}_{-2}$. Dutrey, Guilloteau & Simon (2003) confirm the low inclination, $i = 28^{\rm o} \pm 2^{\rm o}$, but report a PA $= 57^{\rm o} \pm 4^{\rm o}$.

Our data: We have measured a small continuum polarisation of about 0.1% at a PA of approximately 70$^{\rm o}$.

The continuum in the QU plane is not well-defined, due to the low S/N, but the data are good enough to show the presence of a loop in the QU plane. Despite the relative faintness of the object, the loop in the QU plane and the presence of a strong magnetic field, make BP Tau an ideal target for a dedicated spectropolarimetry monitoring program for detailed studies of the magnetically controlled accretion scenario in pre-main sequence stars.

4.2   The connection with the orientation of the global magnetic field

4.2.1   *The foreground polarisation of FU Ori*

For FU Ori, we have measured an intrinsic PA of 45$^{\rm o}$ (Sect. 4.1.4), which is exactly perpendicular to the measured continuum PA at $\simeq 130^{\rm o}$, which is constant over time, cf. Fig. 4. This 90-degree offset makes it highly likely that there is a significant amount of "crossed" polarisation, i.e. the intrinsic and foreground PA are 90 degrees rotated from one another. The reason being that there is substantial extinction towards FU Ori, which makes it unlikely that the foreground polarisation is low. If it is not low, it must have a PA that is 90-degrees rotated from the intrinsic PA, with a level of polarisation larger than that of the intrinsic polarisation. If this were not so, the measured PA could not be perpendicular to the intrinsic one. To be more precise: given the A_V of 1.38 – 2.66 to FU Ori, and using the standard relation between A_V and %P, $\frac{P^{\rm max}}{A_{\rm V}} = 3$, due to Serkowski, Mathewson & Ford (1975), the expected amount of foreground polarisation cannot exceed $\simeq 8$%. Since the measured polarisation is only of the order of $\simeq 1$%, it suggests that the intrinsic P could be up to $\simeq 7$%. We note that these values are maximal and uncertain (due to the uncertainties in the used Serkowski relation), but the inferred 90-degree offset in the PA of the intrinsic and foreground polarisation, in addition to the significant A_V, strongly suggests that the value of the intrinsic polarisation greatly exceeds the measured one. We anticipate that this crossed polarisation is not a coincidence, but that it is related to the star formation process itself (see later).

4.2.2   *The foreground polarisation of DR Tau*

For DR Tau, we have measured an intrinsic PA of 120$^{\rm o}$(Sect. 4.1.6), which is almost parallel to the measured continuum PA at $\simeq 130^{\rm o}-140$ $^{\rm o}$, cf. Fig. 4. Although the

intrinsic and measured PA are parallel for DR Tau, whilst they were perpendicular for FU Ori, the reasoning is the same. QU vector addition of intrinsic and foreground polarisation can either result in a measured polarisation seen in a particular quadrant of the QU plane, or on the opposite quadrant. The consistency between the intrinsic and measured PA could suggest a very low foreground contribution, or, given the A_V of 1.0, more likely to be crossed polarisation – similar to the case of FU Ori. Using the standard relation between A_V and polarisation, one would expect up to 3% foreground polarisation. Since the foreground PA is inferred to be at $\simeq 40°$, whilst the PA of the intrinsic and measured polarisations are at $\simeq 130°$, the intrinsic polarisation may exceed the amount of foreground polarisation by some amount. We argue that this cross-foreground effect for DR Tau is probably as real as for the case outlined above, although the evidence for it is not as strong as for FU Ori, for which its A_V, and hence its expected polarisation is much larger.

5 THE HERBIG AE/BE STARS

The data of the complementary Herbig Ae/Be stars are presented in Figs. 5 and 6, as triplots and loci in the QU plane, for objects that respectively do and do not show line effects. Note that these Herbig Ae/Be star data only represent a fraction of our total Herbig Ae/Be star database that was published in Vink et al. (2002).

5.1 Complementary Herbig Ae/Be star data

5.1.1 MWC 480

MWC 480 was the first Herbig Ae star for which a rotating structure has been detected at longer wavelengths. Mannings et al. (1997) found an inclined disk, $i = 30°$, with a PA $= 157° \pm 4°$. Simon et al. (2000) derive a disk PA and inclination of respectively PA $= 148° \pm 1°$, $i = 38° \pm 1°$. Augereau et al. (2001) do not detect the disk with HST, although they argue for disk rotation over an angular scale of a few arcsec. Eisner et al. (2004) find an inclined disk with PA $\simeq 150°$, $i \simeq 30°$. I.e. all imaging studies agree on a PA of $\simeq 150°$.

Our data: Since we did not detect significant variability in the line polarisation spectra of MWC 480, taken in a few nights of 2001 December, we have combined these data, and obtained a higher S/N. The combined data are shown in Fig. 5. In accordance with the data in Vink et al. (2002), there is an excursion present in the QU plane, consistent with the McLean effect, but there is no detection of a QU loop. The PA of the QU plane excursion is 60°, which is consistent with a 90-degree rotation compared to the above-mentioned imaging and interferometry studies.

5.1.2 MWC 361 = HD 200775

The star is known to be a binary (Li et al 1994; see also Millan-Gabet, Schloerb & Traub 2001), with MWC 361 B positioned at a PA of 164° (see Pirzkal, Spillar & Dyck

1997). Pogodin et al. (2004) present high-resolution spectroscopy to search for periodicity, but these attempts have so far been unsuccessful. Miroshnichenko et al. (1998) report high Hα emission activity, which they claim is recurrent on a 3.68 year timescale.

Our data: We notice complex changes across Hα in the polarisation triplot, accompanied by a complex structure in the QU plane. In Vink et al. (2002) we noted the possibility of the presence of a linear excursion and a loop, which is here confirmed on the basis of higher quality data.

5.1.3 SV Sep

We show the data of SV Cep because of the well-observed loop in the QU plane, the loop is more pronounced than in Vink et al. (2002).

5.1.4 HD 141569

HD 141569 is known to be an object that is transitional between a PMS star and a main sequence star with a debris disk. HST coronographic observations by Augereau et al. (1999) revealed a dust ring that peaks at approximately 325 AU. This disk is found to be inclined at $37.5° \pm 4.5°$ to the line of sight (see also Weinberger et al. 1999; Mouillet et al. 2001). The disk appears to have a central gap extending out to $17 - 30$ AU (Sylvester & Skinner 1996; Marsh et al. 2002; Brittain et al. 2003).

Our data: The polarisation data of HD 141569, shown in Fig. 6, do not indicate a line effect. This could possibly be due to a lack of scattering particles, caused by the large central gap.

5.1.5 MWC 166 (= HD 53367) & GU CMa (= HD 52721)

MWC 166 has shown significant changes in its line depolarisation character, which we have linked to changes in the equivalent width (see Vink et al. 2002). Here, the Hα line is mainly in absorption. Such dramatic changes in the Hα equivalent width are not uncommon for classical Be stars (cf. the extreme case of HD 76534 Oudmaijer & Drew 1997) For completeness, the other Type III (according to Hillenbrand et al. 1992) Herbig Be star that we have re-observed, GU Cma, has not yet shown depolarisations.

5.1.6 AB Aur – not plotted

AB Aur is the brightest Herbig star in the sky and a member of the "B8 – A2 subclass" where P Cygni absorption is more often observed. We have already shown in Vink et al. (2002) that this is often accompanied by the McLean effect.

Mannings & Sargent (1997) have detected a rotating disk of 450 AU in the ^{13}CO (J = 1-0) line, and they derived an inclination of 76° and a PA of 79°. However, Grady et al. (1999) found an upper limit to the inclination of 45° with HST. Eisner et al. (2003) found an inclination $i = 27° - 35°$, and revised this to $i = 8° - 16°$ in Eisner

Table 4. Herbig Ae/Be Targets. The integration times (column 6) denote the total exposures. The continuum PA and its error are indicated in column (8), whilst column (9) indicates whether we have good Hα line polarisation data; the + indicates there is a plot of the epoch. Finally, column (10) indicates a measure of the sky PA derived from line excursions.

Name	V	Spec. Tp	Type of object	Date	Exposure(s)	$P_{\rm cont}^{\rm R}$ (%)	$\Theta_{\rm cont}^{\rm R}$ (°)	Hα data?	$\Theta_{\rm intr}^{\rm R}$
(1)	(2)	(3)	(4)	(5)	(6)	(7)	(8)	(9)	(10)
MWC 480	7.7	A5	HAe	26-12-01	16×75	0.176 ± 0.005	63.0 ± 0.8	yes	55°
				26-12-01	16×30	0.173 ± 0.011	60.2 ± 1.8	yes	
				27-12-01	16×45	0.185 ± 0.006	59.7 ± 1.0	yes	
				27-12-01	8×45,8×90	0.226 ± 0.017	56.9 ± 2.2	yes	
				28-12-01	20×60,8×90	0.281 ± 0.009	61.8 ± 0.9	yes	
				28-12-01	8×45,16×60	0.297 ± 0.010	64.8 ± 1.0	yes	
AB Aur	7.1	A0	HAe	27-12-01	20×30	0.109 ± 0.007	55.3 ± 1.7	yes	
				27-12-01	16×30	0.102 ± 0.008	57.0 ± 2.2	yes	160°
				27-12-01	16×30	0.122 ± 0.007	51.0 ± 1.7	yes	
				10-12-03	4×60,16×90	0.262 ± 0.003	48.2 ± 0.3	yes	
				11-12-03	20×60	0.335 ± 0.003	52.1 ± 0.3	yes	
				13-12-03	4×120,12×90	0.288 ± 0.003	47.5 ± 0.3	yes	
UX Ori	9.6	A4	HAe	27-12-01	4×60	1.825 ± 0.063	112.4 ± 1.0	no	
BF Ori	10.3	A5	HAe	27-12-01	16×180	0.886 ± 0.017	52.0 ± 0.6	no	
LKha 215	10.6	B7.5	HAe	27-12-01	16×120	1.343 ± 0.018	75.9 ± 0.4	no	
HD 141569	7.0	B9.5	HAe	27-12-01	16×120	0.647 ± 0.005	85.2 ± 0.2	yes	
GU Cma	6.6	B2	HBe	10-12-03	4×60	1.726 ± 0.006	27.0 ± 0.1	yes	
				12-12-03	4×20,8×90	1.293 ± 0.011	67.6 ± 0.2	yes	
MWC 166	7.0	B0	HBe	11-12-03	4×20,12×120	0.164 ± 0.003	36.8 ± 0.4	yes	
				12-12-03	4×120	0.394 ± 0.004	35.9 ± 0.3	no	
SV Cep	10.1	A2	HAe	12-12-03	4×60,8×180	1.293 ± 0.011	67.6 ± 0.2	yes	
MWC 361	7.4	B2	HBe	13-12-03	24×30	0.801 ± 0.003	93.6 ± 0.1	yes	(90°)

Table 5. The new Herbig Ae/Be star Hα line results. The errors on the equivalent widths of the Hα lines (column 2) are below 5%, the errors on $\Delta\lambda$(Pol) (column 5) and $\Delta\lambda(I)$ are determined at Full Width Zero Intensity (FWZI) and are about 10%. $\Delta\lambda$(Pol) has been defined as the width over which the polarisation changes. In the case where the widths in PA and %Pol are unequal, we take the largest of the two. The fractional width ($\frac{\Delta\lambda({\rm Pol})}{\Delta\lambda(I)}$) is given in Column (6). The followed recipe with regard to the depolarisation question (column 7) is described in the text. Column (8) represents the morphology in QU space.

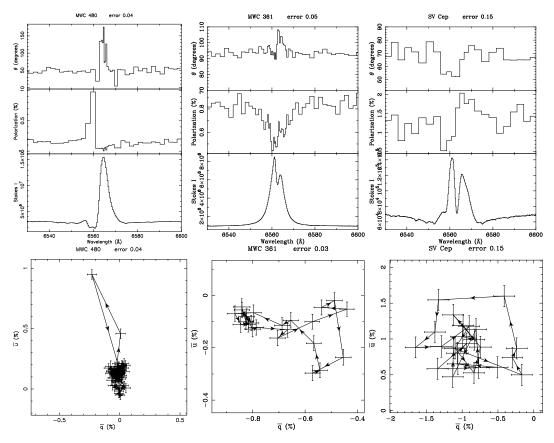| Object	Hα EW(Å)	Line/Cont contrast	Line effect?	$\Delta\lambda$(Pol) (Å)	($\frac{\Delta\lambda({\rm Pol})}{\Delta\lambda(I)}$)	depolarisation?	QU behaviour	Mean character
(1)	(2)	(3)	(4)	(5)	(6)	(7)	(8)	(9)
MWC 480	−21	5.2	Yes			No	exc/loop?	McLean
	−20	5.1	Yes?			No	exc+exc?	
	−22	5.1	Yes			No	–	
	−22	5.1	Yes			No	–	
	−19	4.6	Yes?			No	–	
	−19	4.3	Yes?			No	–	
AB Aur	−33	7.3	No	–	–	–	–	Loop/McLean
	−34	6.9	No	–	–	–	–	
	−34	7.0	Yes?			No	loop?	
	−35	6.9	Yes?			No	loop	
	−34	6.9	Yes?			No	–	
	−30	6.1	Yes?			No	–	
HD 141569	−5.5	1.4	No	–	–	–	–	None
GU Cma	−9.3	2.2	No	–	–	–	–	None
	−9.3					No	–	
MWC 166	+0.59	0.75	No	–	–	–	–	Abs
SV Cep	−11	2.0	Yes?	20	1.0	No	loop	Loop
MWC 361	−47	8.2	Yes			Yes(+)	exc/loop?	Depol+Loop

Figure 5. Triplots and QU plots of 3 Herbig Ae/Be stars that show a line effect.
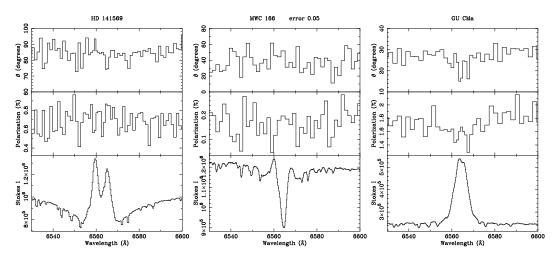

Figure 6. Triplots and QU diagrams of a few Herbig Ae/Be stars without the detection of a line effect.

et al. (2004). Fukagawa et al. (2004) have recently performed coronographic H-band imaging, and these authors derive a disk PA and inclination of respectively PA = $58° \pm 5°$ and $i = 30° \pm 5°$. The apparent inconsistency between the inclination derived from the mm studies and the lower wavelength studies may raise the question of whether the AB Aur disk could be significantly warped. However, recent kinematic modelling of the outer mm disk seems to suggest that the inclination is $\lesssim 30$ degrees (see Natta et al. 2001; Corder, Eisner & Sargent 2005).

Our data: From the McLean effect in Vink et al. (2002) we find an intrinsic PA of $160°$. This is in good agreement with a 90-degree rotation of the PA of the polarisation compared to all above-mentioned imaging and interferometry studies. If we adopt the likely inclination of $\simeq 30°$, we can use the Vink et al. (2005) $i - R_{in}$ table to set a lower limit to the disk inner hole of AB Aur from the presence of the single loop in the QU plane: $R_{in} \gtrsim 5 R_*$.

5.2   A summary of Herbig Ae/Be star PAs

The complementary Herbig Ae/Be star data have not changed the statistics, nor challenged the conclusions reached in Vink et al. (2002). However, since new imaging results with PA and i information have recently become available, we have summarised the new information in the form of Table 6. We have only included sources for which we can infer a well-defined PA of the polarisation from the QU plane, and give more uncertain values in brackets. For most of the T Tauri and some of the Herbig Ae stars, PA information is already available from imaging studies, but for the more massive PMS stars such information is lacking, due to the larger distances involved. Nonetheless, such information may become available, if not spatially resolved, then maybe through interferometric analyses.

In addition to the objects studied in this paper, we draw attention to CQ Tau. VLA data by Testi et al. (2003) suggest the presence of an inclined disk with $i \simeq 70^{\rm o}$. However, Eisner et al. (2004) find the disk inclined with $i \simeq 48^{\rm o}$, at a PA = 104 – 106 °. Kinematic modelling of more sensitive mm data is reported to show that also the outer disk is inclined by $\simeq 45^{\rm o}$ (Corder et al., in preparation).

The data reported in Vink et al. (2002) show the presence of the McLean effect across the *red*-shifted absorption. This occurs at a PA of 20°. Interestingly, this is consistent with a 90° rotation compared to the imaging studies. The reported inclination of $\simeq 45^{\rm o}$ may subsequently again be used to constrain the disk inner hole of CQ Tau: $R_{\rm in} \gtrsim 4$ R_*.

6   DISCUSSION

6.1   The inner disk in PMS stars

One of the motivations behind this study is to discover whether there is a dependence of the circumstellar geometry of PMS stars on stellar mass.

First we restate the raw statistics of the frequency of detectable line effects across Hα among the Herbig Ae/Be and T Tauri stars. We have previously found that about half of the HBe stars have detectable changes across the line (7 out of 12 to be precise), while this rate rises to 9 out of 11 for the HAe stars, and here we find that this fraction is 9/10 for T Tauri stars. In Vink et al. (2002) we showed that in the case of Herbig Ae/Be stars, the fractional widths tend to decrease toward later spectral type (see also Fig. 7). To study whether there is any further dependence on spectral type for T Tauri stars, we have combined the fractional widths with the Herbig data from Vink et al. (2002) and plotted them in Fig. 7. There is much scatter, partly due to the difficulty of measurement and uncertainties in spectral typing, but presumably also due to real physical scatter. Nonetheless, it is apparent that the fractional widths for e.g. the B0-B2 HBe stars are higher than those measured at spectral types later than A2. Vink et al. (2002) found that $(\frac{\Delta\lambda({\rm Pol})}{\Delta\lambda(I)}) = 1.0 \pm 0.2$ for the early Herbig Be (B0 – B2) group. With the new Herbig Ae star data, we have updated the fractional width for the Herbig Ae group to $(\frac{\Delta\lambda({\rm Pol})}{\Delta\lambda(I)}) = 0.7 \pm 0.3$. Finally, for the T Tauri stars, we find $(\frac{\Delta\lambda({\rm Pol})}{\Delta\lambda(I)}) = 0.5 \pm 0.2$.

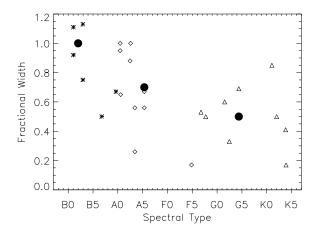Of further significance is that the late Herbig Ae and T Tauri stars present similar characteristics in their Hα line

Figure 7. The fractional width $(\frac{\Delta\lambda({\rm Pol})}{\Delta\lambda(I)})$ plotted against spectral type. The stars indicate the Herbig Be stars, the open diamonds represent the Herbig Ae stars, whilst the T Tauri stars are indicated by open triangles. The errors on the fractional width $(\frac{\Delta\lambda({\rm Pol})}{\Delta\lambda(I)})$ are about 10 per cent. The black circles indicate the averages of the subgroups as discussed in the text.

polarimetry, and this stands in sharp contrast to the Hα depolarisations that are seen in the Herbig Be stars. The depolarisations simply signal a flattened geometry, consistent with an undisrupted disk on small scales, but kinematic information on the inner gas is not obtained. On the other hand, the QU loops found for the Herbig Ae and T Tauri stars are due to intrinsic *line* polarisation that is caused by scattering of a compact source of Hα photons off an exterior rotating disk. It is tempting to associate the presence of a compact source of Hα photons and a rotating undisrupted disk with the magnetospheric accretion scenario, but this is not a required interpretation. Nevertheless, the observed single QU loops, as for instance measured in the magnetically active T Tauri star BP Tau and many other T Tauri and Herbig Ae stars, are consistent with the properties expected of magnetospheric accretion – a model that was proposed to explain a range of phenomena other than those reported here.

From our linear spectropolarimetry data we find additional results which would be hard to obtain from straightforward spectroscopy. In a few cases, most notably FU Ori and DR Tau, we find the McLean effect: an increase in the degree of polarisation across Stokes I absorption, usually seen blueshifted, but it may also be observed in the red wing, cf. CQ Tau. Modeling of these effects may become a worthwhile exercise, given their frequent discovery in strongly accreting objects such as FU Ori. The extra information from the spectropolarimetry may provide vital constraints for understanding disk winds in young stellar objects. Furthermore, the McLean polarisation effects give a particularly accurate value for the intrinsic PA of the polarisation.

We have therefore searched the literature for information on position angles and inclinations of known imaged disks by infrared/millimetre imaging and interferometry. Although there is a lack of imaged disk PAs, there is consistency between the PAs found from our Hα line polarimetry and the larger disks from imaging studies, cf. column (4) in Table 6. For the three Herbig Ae stars with imaged disk

PAs, our polarisation PAs are perpendicular to these larger disk PAs, consistent with the picture of an optically thin inner gaseous disk for Herbig Ae stars . A similar result is found for the F8 T Tauri star RY Tau, but for the later-type T Tauri stars and FU Ori, the imaged disk PAs are aligned with the polarisation PAs – indicating optically thick, multiple scattering inner disks. Although we find the geometry and kinematics of T Tauri and Herbig Ae stars to be very similar, i.e. rotating inner disks, the optical depths of these disks appear to be different. There seems to be a change from optically thick disks in T Tauri stars to optically thin ones for Herbig Ae stars. This appears to be consistent with recent NIR interferometry results (e.g. Monnier et al. 2005). The optically thin disk in Herbig Ae stars may allow the stellar radiation to hit the inner wall of the outer dust disk (located at roughly 1 AU), and to "puff it up" as described by Dullemond, Dominik & Natta (2001).

6.2 The connection with the orientation of the magnetic field in the foreground material

In the basic picture of the star formation process (e.g. Uchida & Shibata 1985), one would expect the stellar accretion disk axis to be parallel to the global magnetic field. Although there are still many uncertainties in the physics of grain alignment (e.g. Roberge & Lazarian 1999), one would normally expect the grains to align perpendicular to the global magnetic field. This would yield foreground polarisation with the observed polarisation PA parallel to this global field. Imaged disks should hence be found perpendicular to the direction of foreground polarisation. At first this was confirmed (e.g. Tamura & Sato 1988), but more recently it has been called into question by Ménard & Duchene (2004), who found the disk orientations in Taurus to be consistent with a random orientation. We have seen in Sect. 4.2 that for those cases where we can infer the PAs of the intrinsic *and* the foreground polarisation, these are 90-degrees rotated from each other. Although the cases where we are able to derive these intrinsic and foreground PAs simultaneously are few at the present time, these data nonetheless hint at an undisturbed star-forming collapse where the orientation of the environment's magnetic field is preserved. If dynamical effects (e.g. Bate, Bonnell & Bromm 2003) are important in nearby star-forming molecular clouds such as Taurus and Orion, this would typically break the connection between the stellar axis and the foreground magnetic field direction – in contradiction to the results currently at hand.

7 CONCLUSIONS

We have presented Hα spectropolarimetry observations of a sample of 10 bright T Tauri stars, supplemented with new Herbig Ae/Be star data. From these data we draw the following conclusions:

• The changes in the linear polarisation across Hα in T Tauri (9/10) and Herbig Ae (9/11) objects are consistent with the presence of a compact source of line emission that is scattered off a rotating inner accretion disk.

• We find consistency between the PA of the polarisation and those of known disk PAs from infrared and millimetre imaging and interferometry studies, that measure larger scales.

• For the Herbig Ae stars, AB Aur, MWC 480 and CQ Tau, and the early-type T Tauri star RY Tau, we find the PA of the polarisation to be perpendicular to the imaged disk – indicative of optically thin inner disks for Herbig Ae stars.

• The polarisation PA is found to be parallel with the imaged disk for the T Tauri stars DR Tau and SU Aur, as well as FU Ori. This is consistent with multiple scatterings in optically thick accretion disks.

• We can constrain the sizes of disk inner holes by combining known inclination angles with the results of Monte Carlo scattering models for the disks of SU Aur ($R_{in} > 3\ R_*$), GW Ori ($R_{in} \simeq 3$–$4\ R_*$), AB Aur ($R_{in} \gtrsim 5\ R_*$), and CQ Tau ($R_{in} \gtrsim 4\ R_*$).

• For FU Ori and DR Tau, we infer the PA of the intrinsic and foreground polarisations to be mutually perpendicular. This suggests an undisturbed star-forming collapse in which a "memory" of the orientation of the large scale magnetic field is preserved.

REFERENCES

Akeson R.L., Koerner D.W., Jensen W.L.N., 1998, ApJ 505, 358
Akeson R.L., Ciardi D.R., van Belle G.T., Creech-Eakman M.J., 2002, ApJ 566, 1124
Akeson R.L., Ciardi D.R., van Belle G.T., 2003, SPIE 4838, 1037
Alencar S.H.P., Johns-Krull C.M., Basri G., 2001, AJ 122, 3335
Angel J.R.P., 1969, ApJ 158, 219
Artymowicz P., Lubow S.H., 1994, ApJ 421, 651
Augereau J.C., Lagrange A.M., Mouillet D., Ménard F., 1999, A&A 350, 51
Augereau J.C., Lagrange A.M., Mouillet D., Ménard F., 2001, A&A 365, 78
Basri G., Martin E.L., Bertout C., 1991, A&A 252, 625
Bastien P., 1982, A&AS 48, 153
Bastien P., 1985, ApJS 59, 277
Bastien P., Landstreet J.D., 1979, ApJ 229, 137
Bastien P., Ménard, 1988 ApJ 326, 334
Bate M.R., Bonnell I.A., Bromm V., 2003, MNRAS 339, 577
Bergner Yu. K., Miroshnichenko A.S., Yudin R.V., Yu N., Yutanov K.G., Dzhakusheva K.G., Mukanov D.B., 1987, PAZh 13, 208
Bouvier J., & Bertout C., 1989, A&A 211, 99
Bouvier J., Bertout C., Benz W., Mayor M., 1986, A&A 165, 110

Brittain S.D., Rettig T.W., Simon T., Kulesa C., DiSanti M.A., Dello Russo N., 2003, ApJ 588, 535

Brown J.C., McLean I.S., 1977, A&A 57, 141

Calvet N., Hartmann L., Kenyon S.J., Whitney B.A., 1994, ApJ 434, 330

Catala C., et al., 1999, A&A 345, 884

Clarke D., McLean I.S. 1974, MNRAS 167, 27

Corder S., Eisner J., Sargent A., ApJL, in press, astro-ph/0502131

DeWarf L.E., Sepinsky J.F., Guinan E.F., Ribas I., Nadalin I., 2003, ApJ 590, 357

Drissen L., Bastien P., St-Louis N., 1989, AJ 97, 814

Dougherty S.M., Taylor A.R., 1992, Nature 359, 808

Dullemond C.P., Dominik C., Natta A., 2001, ApJ 560, 957

Dutrey A., Guilloteau S., Simon M., 2003, A&A 402, 1003

Dyck H.M., Simon T., Zuckerman B., 1982, ApJ 225, 103

Eisner J.A., Lane B.F., Akeson R.L., Hillenbrand L.A., Sargent A.I., 2003, ApJ 588, 360

Eisner J.A., Lane B.F., Hillenbrand L.A., Akeson R.L., Sargent A.I., 2004, ApJ 613, 1049

Folha D.F.M., Emerson J.P., 1999, A&A 352, 517

Fukagawa M., 2004, ApJ 605, 53

Gahm G.F., Gullbring E., Fischerstrom C., Lindroos K.P., Loden K., 1993 A&AS 100, 317

Ghez A.M., Neugebauer G., Gorham P.W., Haniff C.A., Kulkarni S.R., Matthews K., Koresko C., Beckwith S., 1991, AJ 102, 2066

Ghez A.M., Neugebauer G., Matthews K., 2003, AJ 106, 2005

Gómez de Castro A.I., Verdugo E., 2003, ApJ 597, 443

Grady C.A., Woodgate B., Bruhweiler F.C., Boggess A., Plait P., Lindler D.J., Clampin M., Kalas P., 1999, ApJ 523, L151

Greaves J.S., 2004, MNRAS 351 99

Grinin V.P., Kolotilov E.A., Rostopchina A., 1995, A&AS 112, 457

Gullbring E., & Gahm G.F., 1986, A&A 308 821

Hartmann L., 1999, NewAR 43, 1

Hartmann L., Kenyon S.J., 1985, ApJ 299, 462

Hartmann L., Hewett R., Stahler S., Mathieu R.D., 1986, ApJ 309, 275

Heines A., Henning T., Szeifert T., 1997, IAUS 182, 294

Herbig G.H., 1977, ApJ 217, 693

Herbig G.H., Bell R.K., 1988, Lick Observatory Bulletin, 1111

Herbst W., et al., 1987, AJ 94, 137

Hillenbrand L.A., Strom S.E., Vrba F.J., Keene J. 1992, ApJ 397, 613

Hogerheijde M.R., van Langevelde H.J., Mundy L.G., Blake G.A., van Dishoeck E.F., 1997, ApJ 490, 99

Hough J.H., Bailey J., Cunningham E.C., McCall A., Axon D.J., 1981, MNRAS 195, 429

Johns C.M., Basri G., 1995, AJ 109 2800

Johns-Krull C.M., Valenti J.A., Koresko C., 1999, ApJ 516, 900

Kitamura Y., Momose M., Yokogawa S., Kawabe R., Tamura M., Ida S., 2002, ApJ 581, 357

Koerner D.W., Sargent A.I., 1995, AJ 109, 2138

Koresko C.D., 2000, ApJ 531, 147

Kravtsova A.S., Lamzin S.A., 2002, AstL 28, 676

Lamzin S.A., Shevchenko V., Grankin K., Mel'nikov S., 1998, Ap&SS 261, 167

Li W., Evans N.J., Harvey P.M., Colome C., 1994, ApJ 433, 199

López-Martín L., Cabrit S., Dougados C., 2003, A&A 405

Malbet F., et al., 1998, ApJ 507, 149

Malbet F., et al., 2005, A&A submitted

Mannings V., Sargent A.I., 1997, ApJ 490, 792

Mannings V., Koerner D.W., Sargent A.I., 1997, Nature 388, 555

Marsh, K.A., Silverstone M.D., Becklin E.E., Koerner D.W., Werner M.W., Weinberger A.J., Ressler M.E., 2002, ApJ 573, 425

Mathieu R.D., Adams F.C., Latham D.W., 1991, AJ 101, 2184

Mathieu R.D., Adams F.C., Fuller G.A., Jensen E.L.N., Koerner D.W., Sargent A.I., 1995, AJ 109, 2655

McKee C.F., Tan J.C., 2003, ApJ 585, 850

McLean I.S., 1979, MNRAS 186, 265

Ménard F., Bastien P., 1992, AJ 103, 564

Ménard F., Duchêne G., 2004, A&A 425, 973

Millan-Gabet R., Schloerb F.P., Traub W.A., 2001, ApJ 546, 358

Miroshnichenko A.S., Mulliss C.L., Bjorkman K.S., Morrison N.D., Glagolevskij Y.V., Chountonov G.A., 1998, PASP 110, 883

Monnier J.D., Millan-Gabet R., Billmeier R., Akeson R., Wallace D., et al., 2005, ApJ in press, astro-ph/0502252

Mora A., et al., 2001, A&A 378, 116

Mouillet D., Lagrange A.M., Augereau J.C., Ménard, F., 2001, A&A 372, 61

Mundt R., Walter F.M., Feigelson E.D., Finkenzeller U., Herbig G.H., Odell A.P., 1983, ApJ 269, 229

Murdin P., Penston M.V., 1977, MNRAS 181, 657

Muzerolle J., Calvet N., Hartmann L., 2001, ApJ 550, 944

Najita J., Carr J.S., Mathieu R.D., 2003, ApJ 589, 931

Natta A., Prusti T., Neri R., Wooden D., Grinin V.P., Mannings V., 2001, A&A 371, 186

Oudmaijer R.D., Drew J.E., 1997, A&A 318, 198

Oudmaijer R.D., Drew J.E. 1999, MNRAS 305, 166

Oudmaijer R.D., et al., 2001, A&A 379, 564

Petrov P.P., Gahm G.F., Gameiro J.F., Duemmler R., Ilyin I.V., Laakkonen T., Lago M.T.V.T., Tuominen I., 2001, A&A 369, 993

Pirzkal N., Spillar E.J., Dyck H.M., 1997, ApJ 481, 392

Poeckert R. 1975, ApJ 152, 181

Poeckert R., Marlborough J.M., 1976, ApJ 206, 182

Pogodin M.A., et al., 2004, A&A 417, 715

Quirrenbach A., et al., 1997, ApJ 479, 477

Roberge W.G., Lazarian A., 1999, MNRAS 305, 615

Rucinski S.M., 1985, AJ 90, 2321

Schulte-Ladbeck R.E., 1983, A&A 120, 203

Serkowski K., 1969, ApJ 156, 55

Serkowski K., Mathewson D.L., Foid V.L., 1975, ApJ 196, 261

Shevchenko V., Grankin K.N., Mel'Nikov S.Y., Lamzin S.A., 1998, PAZh, 24, 614

Simon M., Dutrey A., Guilloteau S., 2000, ApJ 545, 1034

Smirnov D.A., Fabrika S.N., Lamzin S.A., Valyavin G.G., 2003, A&A 401, 1057

Smith K.W., Lewis G.F., Bonnell I.A., Bunclark P.S., Emerson J.P., 1999, MNRAS 304, 367

Stassun K., Wood K., 1999, ApJ 510, 892

Sylvester R.J., Skinner C.J., 1996, MNRAS 283, 457

Symington N.H., Harries T.J., Kurosawa R., Naylor T., 2005, MNRAS, in press

Tamura M., Sato S., 1988, AJ 98, 1368

Testi L., Natta, A., Shepherd D.S., Wilner D.J., 2003, A&A 403, 323

Uchida Y., Shibata K., 1985, PASJ 37, 515

Unruh Y.C., et al., 2004, MNRAS 348, 1301

Vardanyan R.A., 1964, SoByu 35, 3

Vink J.S., Drew J.E., Harries T.J., Oudmaijer R.D., 2002, MNRAS 337, 356

Vink J.S., Drew J.E., Harries T.J., Oudmaijer R.D., Unruh Y.C., 2003, A&A 406, 703

Vink J.S., Harries T.J., Drew J.E., 2005, A&A 430, 213

Wang H., Apai D., Henning T., Pascucci I., 2004, ApJ 601, 83

Weinberger A.J., Becklin E.E., Schneider G., Smith B.A., Lowrance P.J., Silverstone M.D., Zuckerman B., Terrile R.J., 1999, ApJ 525, 53

Wood K., Brown J.C., Fox G.K., 1993, A&A 271, 492

Wood K., Bjorkman K.S., Bjorkman J.E., 1997, ApJ 477, 926

Yudin R.V., 2000, A&AS 144, 285

Table 3. Previous continuum polarimetry. Columns (2) and (3) give the number of measurements and the wavelength at which the polarisation was measured. Columns (4) and (4) list the ranges (not errors) of measured %Pol and PA. The references are given in column (6) and listed below the table.

Object (1)	Number of meas (2)	Lambda (Å) (3)	P_{cont} (%) (4)	Θ_{cont} (°) (5)	Ref (6)
RY Tau	16	5895	1.45 − 3.71	−4 − + 41	1
	14	7543	0.29 − 3.89	−25 −+ 45	1
	3	5500	1.7 − 3.1	18 − 42	2
	2	6800	2.4 − 3.1	22 − 39	2
	3	5500	5.13 − 5.47	35 − 38	3
	3	6800	4.52 − 4.98	33 − 36	3
	3	5895	2.98 − 3.13	17 − 20	4
	1	6800	4.0	14	5
	7	6800	2.48 − 4.03	17 − 26	6
T Tau	8	5895	0.94 − 1.53	95 − 100	1
	7	7543	0.84 − 1.50	94 − 101	1
	3	5500	0.75 − 1.2	90 − 98	2
	2	6800	0.65 − 1.14	91 − 95	2
	1	5895	0.75	100	4
SU Aur	4	5895	0.09 − 0.21	106 − 175	1
	3	7543	0.09 − 0.35	101 − 142	1
	2	5500	0.13 − 0.25	119 − 138	2
	1	6800	0.11	98	2
	3	5500	0.48 − 0.66	127 − 132	3
	3	6800	0.46 − 0.58	119 − 128	3
	1	5895	0.57	103	4
FU Ori	7	5895	0.68 − 0.83	125 − 135	1
	7	7543	0.68 − 0.83	127 − 133	1
CO Ori	1	5895	1.61	6.1	1
	1	7543	1.59	6.1	1
	1	5895	2.76	178	4
	8	6800	1.75 − 2.60	156 − 169	6
DR Tau	1	5500	1.28	140	3
	1	6800	1.1	139	3
	3	5250	0.38 − 0.59	124 − 152	7
	4	6800	0.52 − 0.81	125 − 139	6
RW Aur	2	5895	0.68 − 1.44	53 − 94	1
	2	7543	0.68 − 0.85	49 − 104	1
	3	5500	0.6 − 0.9	101 −103	2
	2	6800	0.8 − 0.9	98 − 102	2
	4	5500	0.45 − 1.12	78 − 105	3
	4	6800	0.41 − 0.92	82 − 100	3
	1	5895	0.79	77	4
GW Ori	1	5895	0.21	102.6	1
	1	7543	0.35	102.0	1
	1	5500	0.52	131	2
	1	6800	0.5	116	2
	1	5895	2.64	151	4
UX Tau	1	5895	0.45	68	4
BP Tau	2	5895	0.17 − 0.36	83.7	1
	2	7543	0.19 − 0.29	69 − 80	1
	1	5895	0.31	93	4

[1] Bastien (1982) [2] Hough et al. (1981) [3] Schulte-Ladbeck (1983) [4] Bastien (1985) [5] Bergner et al. (1987) [6] Oudmaijer et al. (2001) [7] Drissen et al. (1989)

Table 6. Comparison (column 5) between intrinsic position angles of the polarisation (column 3) and those from imaging studies (column 4) for Herbig Ae/Be stars (above) and T Tauri stars (below). The polarisation PA data is taken from Vink et al. (2002,2003) and the present study. Uncertain PA data is given in brackets. Note the lack of imaged disk PAs, especially for the Herbig stars.

Name	Spec. Type	Polarisation PA	Imaging PA	Δ PA
MWC 137	Be	25		
MWC 166	B0	50		
MWC 361	B2	(90)		
BD+40 4124	B2	83		
HD 45677	B3	≃70		
MWC 158	B9	135		
HD 58647	B9	20		
AS 477	B9.5	110		
MWC 120	A0	90		
KMS 27	A0	(65)		
MWC 789	A0	175		
AB Aur	A0	160	60-80[2]	80 − 100
SV Cep	A2	(100)		
XY Per	A2	(70)		
HD 244604	A3	≃155		
T Ori	A3	20		
HD 245185	A5	≃40		
MWC 480	A5	55	150[1]	95
CQ Tau	F2	20	105[3]	95
CO Ori	F7	(60)		
RY Tau	F8	163	62[4]	101
SU Aur	G2	130	127[5]	3
FU Ori	G3	45	47[6]	2
GW Ori	G5	(60)	56[8]?	(4?)
UX Tau A	K2	140		
RW Aur A	K3	115		
DR Tau	K5	120	128[7]	8

[1] Eisner et al. (2004), Mannings et al. (1997), Simon et al. (2000) [2] Fukagawa et al. (2004), Corder et al. (2005) [3] Eisner et al. (2004) [4] Akeson et al. (2003), Koerner & Sargent (1995), Kitamura et al. (2002) [5] Akeson et al. (2002) [6] Malbet et al. (2005) [7] Kitamura et al. (2002) [8] Mathieu et al. (1995)